

Higher Dimensions in High Energy Collisions

A.V. Kisselev

Institute for High Energy Physics, Protvino, Russia

Abstract

Different possibilities of a detection of signals from extra space dimensions at high energy colliders are reviewed.

1 Introduction

In particle physics all the fundamental laws are formulated in 4-dimensional Minkowski space-time. The relativistic SM fields interact at distances $R \lesssim m_{EW}^{-1}$, where $m_{EW} \sim 10^3 \text{ GeV}$ is the electroweak scale. The fluctuations of the underlying metric provide us with a gravitational dynamics. However, the gravity becomes strong only at the Planck scale $M_{Pl} \sim 10^{19} \text{ GeV}$. The first attempt to unify gravity and particle (electromagnetic) interactions traces back to pioneering papers by T. Kaluza and O. Klien [1]. They have given a theoretical framework for a description of particle interactions in a multi-dimensional space-time. The extra space dimensions are strongly motivated by the string and M-theory [2].

The large volume of the extra dimension can explain the hierarchy between the electroweak and Planck scale [3]. The fundamental scale of the gravity may be of the order of several TeV, if a number of additional space dimensions is large enough. A lot of theoretical studies of an underlying theory in the extra dimensions have been done (see, for instance, reviews [4] and references therein). It is important that physical schemes with the extra dimensions result in distinctive phenomenological predictions which can be checked at the LHC or at high energy linear e^+e^- colliders.

In the present mini-review we consider concrete models with the additional compactified dimensions (both with flat and warp metric). In all

of them Kaluza-Klein (KK) massive excitations of the graviton are present which can be produced at TeV's energies. Some of the models provide us with KK states of the SM gauge bosons, Higgs or matter fields. The production and decays of new scalar particles are also described. Finally, we consider a black holes formation which can cloak hard perturbative scattering processes behind a horizon of colliding particles.

Our main goal is a collider phenomenology. That is why we do not consider corrections to a gravitational potential from the KK excitations, as well as astrophysical and cosmology constraints. Such problems as a gauge coupling unification, supersymmetry breaking, neutrino masses and mixing, proton decay, flavor violation *etc.* are also disregarded. Because of the paper size limitation, we present an illustrative material mainly for the LHC, although experimental signatures of the extra dimensions at e^+e^- colliders are discussed in the text. The list of references on the collider phenomenology within the framework of the extra dimensions is not complete. An interested reader can find more references in reviews [5, 6].

2 Large extra dimensions

2.1 ADD model

The large extra dimensions scenario has been postulated by Arkani-Hamed, Dimopoulos and Dvali (ADD) [3] The metric for this model looks like

$$ds^2 = g_{\mu\nu}(x) dx^\mu dx^\nu + \eta_{ab}(x, y) dy^a dy^b, \quad (1)$$

where $\mu, \nu = 0, 1, 2, 3$ and $a, b = 1, \dots, d$. All d extra dimensions are compactified with a characteristic size R_c .

There is a relation between a fundamental mass scale in D dimensions, M_D , and 4-dimensional Planck mass, M_{Pl} :

$$M_{Pl} = V_d M_D^{2+d}, \quad (2)$$

where V_d is a volume of the compactified dimensions. $V_d = (2\pi R_c)^d$ if the extra dimensions are of a toroidal form. In order to get $M_D \sim \text{TeV}$, the radius of the extra dimensions should be large. The compactification scale R_c^{-1} ranges from 10^{-3} eV to 10 MeV if d runs from 2 to 6.

As we see, $R_c \gg m_{EW}^{-1}$. So, all Standard Model (SM) gauge and matter fields are to be confined to a 3-dimensional brane embedded into a $(3 + d)$ -dimensional space (gravity alone lives in the bulk). It means, in particular, that the energy-momentum tensor of matter is of the form

$$T_{AB}(x, y) = \eta_A^\mu \eta_B^\nu T_{\mu\nu}(x) \delta(y), \quad (3)$$

with $A, B = 0, 1, \dots, 3 + d$.

In linearized quantum gravity we have

$$g_{AB} = \eta_{AB} + \frac{2}{M_D^{1+d/2}} h_{AB}(x, y). \quad (4)$$

Performing the KK mode expansion of the gravitational field $h_{AB}(x, y)$, we obtain the graviton interaction Lagrangian

$$\mathcal{L} = -\frac{1}{\bar{M}_{Pl}} G_{\mu\nu}^{(n)} T^{\mu\nu}, \quad (5)$$

where n labels the KK excitation level and $\bar{M}_{Pl} = M_{Pl}/\sqrt{8\pi}$ is a reduced Planck mass. One can conclude from (5) that the coupling of both massless and massive graviton is universal and very small ($\sim 1/\bar{M}_{Pl}$).

The masses of the KK graviton modes are

$$m_n = \frac{\sqrt{n_a n^a}}{R_c}, \quad n_a = (n_1, n_2 \dots n_d). \quad (6)$$

So, a mass splitting is $\Delta m \sim R_c^{-1}$ and we have an almost continuous spectrum of the gravitons.

At energies $E \gg R_c^{-1}$, the multiplicity of states which can be produced is $N(E) \sim (ER_c)^d$. Due to a large phase space, the cross-section of a process involving the production of the KK gravitons with masses $m_n \leq E$ is

$$\sigma_{KK} \sim \frac{1}{\bar{M}_{Pl}^2} N(E) \sim \frac{E^d}{M_D^{d+2}}, \quad (7)$$

that is, it turns out to be measurable at future colliders.

The lifetime of the massive graviton is equal to [7]

$$\tau_n = \frac{1}{M_{Pl}} \left(\frac{M_{Pl}}{m_n} \right)^3. \quad (8)$$

Thus, the KK gravitons behave like massive, almost stable non-interacting spin-2 particles. Their collider signature is an imbalance in missing mass of final states with a continuous mass distribution.

2.2 Direct production of gravitons at colliders

The leading experimental signal of the graviton production at the LHC originates from the process $pp \rightarrow \text{jet} + \cancel{E}_T$ (the subprocess $qg \rightarrow qG^{(n)}$ gives the largest contribution). The main background is $pp \rightarrow Z + \text{jet}$ ($Z \rightarrow \nu\bar{\nu}$). The signal and background rates are shown in Fig. 1 (for the total luminosity $\mathcal{L} = 100 \text{ fb}^{-1}$) [8].

Another signal for the direct production of the massive gravitons is the process $pp \rightarrow \gamma + \cancel{E}_T$ [8]. SM background comes mainly from $pp \rightarrow Z + \gamma$ ($Z \rightarrow \nu\bar{\nu}$). Should graviton be discovered in the jet channel, this process can be used as an independent test, although it has the much lower rate [8].

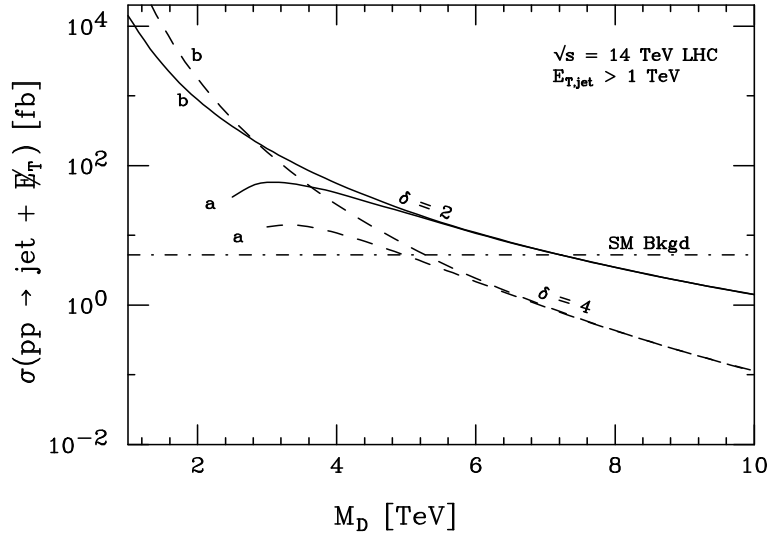


Figure 1: The total jet + nothing cross-section versus M_D at the LHC integrated for all $E_{T,\text{jet}} > 1 \text{ TeV}$ with the requirement that $|\eta_{\text{jet}}| < 3.0$. The SM background is the dash-dotted line, and the signal is plotted as solid and dashed lines for $\delta = 2$ and 4 extra dimensions. The a (b) lines are constructed by integrating the effective energy in the parton collision over $\hat{s} \leq M_D^2$ (all \hat{s}) [8].

The reach limit for Tevatron Run II ($E_{T,\text{jet}} > 150 \text{ GeV}$ and $\mathcal{L} > 300 \text{ fb}^{-1}$) was estimated to be $M_D = 1 \text{ TeV}$ if $2 \leq d \leq 4$.

The graviton production can be also searched for at the future linear colliders in the reaction $e^+e^- \rightarrow G^{(n)} + \gamma/Z$, by analyzing both the total cross section and the angular distribution of final states. SM background comes

predominantly from the process $e^+e^- \rightarrow \nu\bar{\nu}\gamma$. The discovery possibility of e^+e^- collider with $\sqrt{s} = 800 \text{ GeV}$ and $\mathcal{L} = 1000 \text{ fb}^{-1}$ for different values of d and beam polarizations can be found in [8] and [5].

Let us note that the KK excitation signature in the ADD model are quite different from the SUSY signature. The latter is a fixed invisible mass signal accompanied by a variety of leptons, photons and hadron activity.

2.3 Virtual graviton exchange

At tree-level, the contribution of virtual massive gravitons to a matrix element is proportional to

$$\mathcal{M} \sim \frac{i\pi^2}{M_{Pl}^2} \sum_n \frac{1}{s - m_n^2}. \quad (9)$$

The sum in (9) diverges for $d \geq 2$, the cutoff M_H is to be calculated in a full theory. In the string theory it should be related to a string scale M_s and can be less than M_D .

The following (rather rough) substitution is usually made for phenomenological purposes:

$$\mathcal{M} \sim \frac{\lambda}{M_H^4}, \quad \lambda = \pm 1. \quad (10)$$

In hadron collisions the process $pp \rightarrow G^{(n)} \rightarrow \gamma\gamma$ has advantages as it allows to investigate a signal in different domains of the parton subprocess energy. The diphoton and Drell-Yan production ($pp \rightarrow G^{(n)} \rightarrow l^+l^-$) lead to sensitivity of M_H up to 7.4 TeV.

At linear colliders one of the promising reactions is $e^+e^- \rightarrow \gamma\gamma$ [8]. The indirect effects of the massive gravitons can be also examined in the fermion pair production ($e^+e^- \rightarrow G^{(n)} \rightarrow f\bar{f}$). It provides bound $M_H \lesssim 6.6 \text{ TeV}$ (for $\sqrt{s} = 1 \text{ TeV}$) [9]. The angular distributions for the fermion pair production in e^+e^- collisions (say, left-right asymmetries in $e^+e^- \rightarrow b\bar{b}$) can provide a unique signature for spin-2 exchanges. Recently a new technique was proposed which enables one to uniquely isolate the KK gravitons from other possible new states in the process $e^+e^- \rightarrow f\bar{f}$ ($f \neq e$) [10]. It allows to detect the graviton exchange contributions for mass scales up to $6\sqrt{s}$.

3 Warp extra dimensions

3.1 Randall-Sandrum (RS) model

This scenario has been proposed in [11]. The RS model is a model of gravity in a 5-dimensional Anti-de Sitter space with a single extra dimension compactified to the orbifold S^1/Z_2 . The metric has the form

$$ds^2 = e^{-2k|y|} \eta_{\mu\nu} dx^\mu dx^\nu + dy^2, \quad (11)$$

where $y = r_c \theta$ ($0 \leq \theta \leq \pi$), r_c being a "radius" of the extra dimension. The parameter k defines the scalar (negative) curvature of the space.

From the 5-dimensional action one can derive the relation

$$\bar{M}_{Pl}^2 = \frac{M_5^3}{k} (1 - e^{-2kr_c\pi}), \quad (12)$$

which means that $k \sim \bar{M}_5 \sim \bar{M}_{Pl}$.

There are two 3-dimensional branes in the model with equal and opposite tension located at the point $y = \pi r_c$ (so-called the TeV brane) and at $y = 0$ (referred to as the Plank brane). All SM fields are constrained to the TeV brane, while gravity propagates in the additional dimension.

Using a linear expansion of the metric

$$g_{\mu\nu} = e^{-2ky} \left(\eta_{\mu\nu} + \frac{2}{M_5^{3/2}} h_{\mu\nu} \right) \quad (13)$$

and a decomposition of the graviton field in KK modes, we get the interaction of the gravitons with the SM fields

$$\mathcal{L} = -\frac{1}{\bar{M}_{Pl}} T^{\mu\nu} h_{\mu\nu}^{(0)}(x) - \frac{1}{\Lambda_\pi} T^{\mu\nu} \sum_n h_{\mu\nu}^{(n)}(x) \quad (14)$$

with $\Lambda_\pi = \bar{M}_{Pl} e^{-kr_c\pi}$. We see that couplings of all massive states are only suppressed by Λ_π^{-1} , while the zero mode couples with usual strength, \bar{M}_{Pl}^{-1} . The physical scale on the TeV brane, Λ_π , is of the order of 1 TeV for $kr_c \sim 12$.

The masses of the graviton KK excitations are given by

$$m_n = kx_n e^{-kr_c\pi}, \quad (15)$$

where x_n are the roots of the Bessel function $J_1(x)$. It means that the KK gravitons are not equally spaced, contrasted to the ADD model. Thus, a basic signature of the RS model is a resonance production.

Note that in two other RS-type models with infinitely large 5-th dimension [12] there is a continuum of the graviton KK modes.

3.2 Production of light gravitons

For a phenomenological analysis of the RS model, the range $0.01 \lesssim k/\bar{M}_{Pl} \lesssim 0.1$ is usually used. From theoretical considerations it follows that $\Lambda_\pi \lesssim 10$ TeV. The mass of the first excitation is expected to be $m_1 \sim 1$ TeV.

The cleanest signal of the resonance production at the LHC could be an excess in Drell-Yan process ($q\bar{q}, gg \rightarrow G^{(1)} \rightarrow l^+l^-$) [13]. Notice that gg initiated process now contributes to the pair production. The main background processes are $pp \rightarrow G^{(1)} \rightarrow Z/\gamma^* \rightarrow l^+l^-$. It was calculated that the lightest graviton excitation would be seen if $m_1 \lesssim 2.1$ TeV [14].

The dijet production ($q\bar{q}, gg \rightarrow G^{(1)} \rightarrow q\bar{q}, gg$) is expected to have large QCD background. Should the first graviton resonance be discovered at the LHC, all fundamental parameters of the model are determined through its mass m_1 and total width Γ_1 by using the relations:

$$\Lambda_\pi = m_1 \frac{\bar{M}_{Pl}}{kx_1}, \quad \Gamma_1 = \rho m_1 x_1^2 \left(\frac{k}{\bar{M}_{Pl}} \right)^2, \quad (16)$$

where ρ is a number of open channels for $G^{(1)}$ decay.

The tower of narrow s-channel resonances can be seen in $e^+e^- \rightarrow \mu^+\mu^-$. The corresponding cross section as a function of energy \sqrt{s} is presented in Fig. 2 [5]. Such resonances are easily distinguishable from other new states (Z' , for instance) by analyzing the angular distribution of the decay products.

The light graviton can be also produced in association with the photon: $e^+e^- \rightarrow G^{(1)} + \gamma$. Contrary to large extra dimension scheme, we expect a monoenergetic photon here.

As for virtual exchange of the massive gravitons, the corresponding sum has no divergences. Constraints in the $\Lambda_\pi - k/\bar{M}_{Pl}$ plane have been calculated in [13] from the angular distributions in (unpolarized and polarized) e^+e^- annihilation, by summing over e, μ, τ, c and b final states.

Summary of experimental and theoretical constraints on the parameters of RS model with the SM fields lying on the brane, can be found in [15].

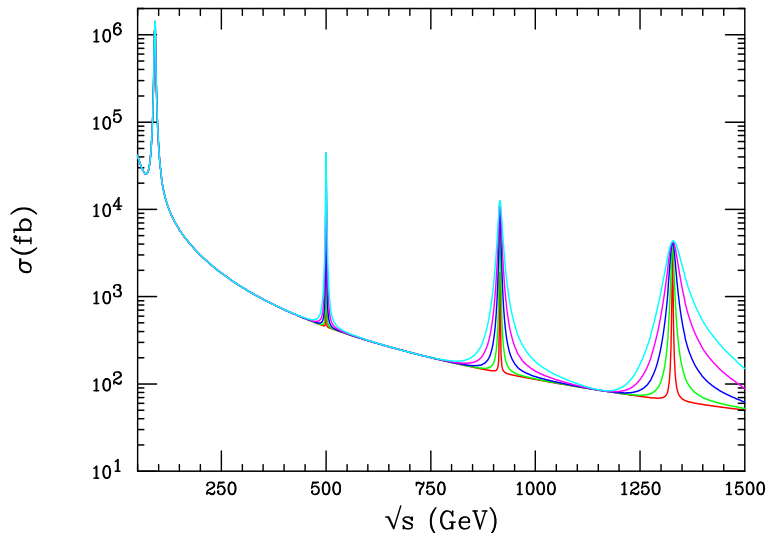


Figure 2: The cross section for $e^+e^- \rightarrow \mu^+\mu^-$ including the exchange of a KK tower of gravitons in the Randall-Sundrum model with $m_1 = 500$ GeV. The curves correspond to the range $k/\overline{M}_{\text{Pl}} = 0.01 - 0.05$ [5].

4 TeV^{-1} Size Extra Dimensions

In the content of the string theory it has been demonstrated that an extra dimension may have size of the order $R_c \sim \text{TeV}^{-1}$, if the fundamental (string) scale is close to 1 TeV [2]. If the SM gauge bosons are allowed to propagate in this compact extra dimension, their light KK excitations have masses $m_A \sim R_c^{-1} \sim 1 \text{ TeV}$. As a result, the relations between electroweak observables will be changed.

There are two kinds of effects. The first one is related to a mixing between zero and KK modes of the W and Z bosons, that results in changes of the masses of the gauge bosons and modification of their couplings to the fermions. The second effect is an extra contribution from a virtual exchange of the KK tower of the gauge bosons. These effects depend on the Higgs field, which may live in the bulk, on the walls, or can be a combination of fields of both types [17, 18].

4.1 5DSM model

This model is an extension of the SM to the 5D flat space. The 5-th dimension y is compactified on the orbifold S^1/Z_2 which has two fixed points at $y = 0$ and $y = \pi R_c$. The SM gauge fields propagate in the 5D bulk, while the chiral matter is localized on the 4D boundaries (so-called walls) [16]. The gravity can live in more extra dimensions than the gauge fields do.

There are two Higgs doublets, ϕ_b and ϕ_w , living in the bulk and on the wall, respectively. Their vacuum expectations are parameterized as follows

$$\phi_b = v \cos \beta, \quad \phi_w = v \sin \beta, \quad (17)$$

where v is the standard VEV. The masses of the lightest gauge bosons ($A = W, Z$) are [17]

$$m_A^{(0)2} = m_A^2 \left(1 - 2 \sin^4 \beta \sum_{n=1}^{\infty} \frac{m_A^2}{n^2 M_c^2} \right), \quad (18)$$

where $M_c = R_c^{-1} \gg m_A$. The couplings of zero modes of the W and Z bosons to the fermions have analogous corrections. The KK excitations acquire the masses

$$M_A^{(n)2} = n^2 M_c^2 + O(m_A^2), \quad n \geq 1. \quad (19)$$

The coupling of the KK excitations to the SM fermions is enhanced by a factor $\sqrt{2}$ with respect to the zero mode coupling g . The more accurate calculations indicate, however, that the gauge couplings to the matter, g_n , are not universal and $g_n \sim g \exp(-An^2/(R_c M_s)^2)$, where M_s is the string scale and A is some constant [19].

The complete analysis of the EW data gives the lower bound $M_c \gtrsim 3.3 - 3.8$ TeV, depending on the value of $\tan \beta$ [18] (see also Refs. [20]).

The states with masses not much larger than 4 TeV may be observable at the LHC. The first excitations of the gauge bosons can be directly produced in Drell-Yan processes mediated by the first KK modes of the gauge bosons, $pp \rightarrow Z^{(1)}/\gamma^{(1)} \rightarrow l^+ l^-$. The second level excitations are too massive to be seen even at the LHC. The analysis is based on a search for a narrow dilepton mass excess. The typical cross section can be seen in Fig. 3.

To see a direct $W^{(1)}$ production, one have to search for a high-energy lepton plus a large missing energy. The SM background can be significantly reduced by cuts. The reach probabilities of the LHC are $M_c \lesssim 5.9(6.3)$ TeV for the $Z^{(1)}/\gamma^{(1)}$ ($W^{(1)}$) channel, respectively [21] (see also estimates from Ref. [22]).

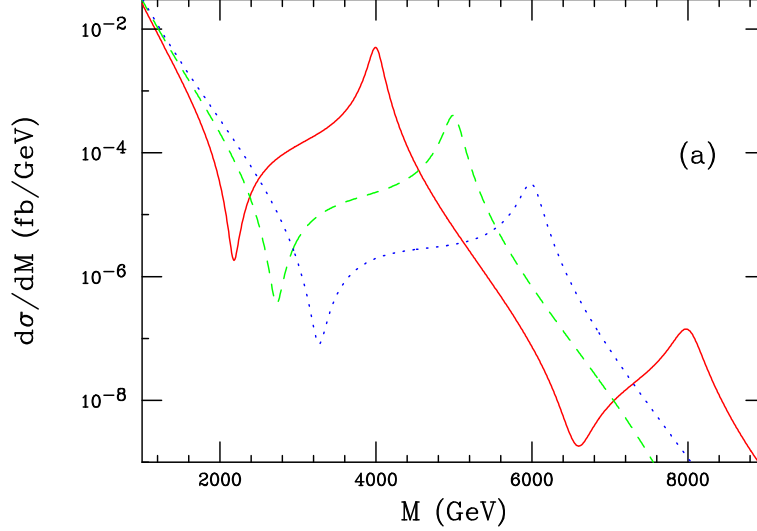


Figure 3: Cross section for Drell-Yan production of the degenerate neutral KK excitations $Z^{(n)}$ and $\gamma^{(n)}$ as a function of the dilepton invariant mass at the LHC assuming one extra dimension with $1/R_c=4(5, 6)$ TeV corresponding to the solid (dashed, dotted) curve. The second excitation is only shown for the case of $1/R_c = 4$ TeV [18].

The LHC will not be able to distinguish degenerate pair of the first excitation of Z and γ from an ordinary Z' when quarks and leptons are not at the same wall. This ambiguity can be resolved by e^+e^- collider with energy \sqrt{s} much below the masses of KK excitations. As for their values, a linear collider with $\sqrt{s} = 1(1.5)$ TeV can probe KK particles up to 23(31) TeV if integrated luminosity 500 fb^{-1} is obtained [18]. This limit is set by the total rates and polarization asymmetries of the processes $e^+e^- \rightarrow Z^{(n)}/\gamma^{(n)} \rightarrow f\bar{f}$ for all accessible fermions.

It is interesting to note that the bulk Higgs ($\tan\beta = \infty$) can be as large as $m_h = 500$ GeV in the 5DSM, while for the wall Higgs scenario ($\tan\beta = 0$) the value $m_h \leq 260$ GeV is favored by the EW data.

4.2 RS model with bulk gauge fields

Here we consider the case of gauge bosons propagating in the slice of AdS_5 (see the previous section for details of the warp metric). The fermions are located on the TeV brane.

In the limit $m_n \ll k$, the masses of the gauge bosons are

$$m_n \simeq kx_n e^{-kr_c\pi}, \quad (20)$$

where x_n are the roots of the Bessel function $J_0(x)$ [23]. As was shown in [13], the KK excitations of the gauge bosons are essentially lighter than the graviton excitations of the same level n .

The ratio of the scale coupling constant of the KK mode, g_n and zero mode, g , is equal to

$$\frac{g_n}{g} = \sqrt{2\pi k r_c}, \quad n \geq 1. \quad (21)$$

Putting $kr_c \simeq 11.27$, we get $\sqrt{2\pi k r_c} \simeq 8.4$. It means that the KK modes couple to the 3D matter fermions about 8 times stronger than the zero mode does. Therefore, one should expect that the tower exchange gives more significant contribution to the EW observables than in the case with the bulk gauge bosons living in the flat metric.

Actually, the constraint on the mass of the first excitation was estimated to be $m_1 \gtrsim 23$ TeV, while $\Lambda_\pi \gtrsim 100$ TeV [24]. In Ref. [25] lower bounds on the size of the extra dimension, πr_c , and on the masses of the KK excitations were calculated as functions of the Higgs mass m_h . In particular, for $m_h = 115$ GeV it was obtained that $(\pi r_c)^{-1} > 11$ TeV, $m_1^W \gtrsim 27$ TeV and $m_1^G \gtrsim 46$ TeV. For the heavy Higgs with the mass $m_h = 600$ GeV, the limits look like $8.2 < (\pi r_c)^{-1} < 22$ TeV. Thus, one can conclude that in the RS model with the bulk gauge fields, resonances of both gauge bosons and gravitons lie far beyond the reach of the the LHC.

Recently, the more complicated space-time background of the form $AsS_5 \times \mathcal{M}^\delta$, where \mathcal{M}^δ is an orbifold with δ dimensions, was considered [26]. For the flat orbifold S^1/Z_2 a multitude of the KK graviton states appears. Moreover, couplings of different modes are measurably non-universal, if $kR \sim 1$, where R is the radius of the S^1 .

In another paper [27], the effect of boundary kinetic terms is investigated. The substantial suppression of the couplings of the KK gauge states was found. It means that the lightest KK particles are of the order of a few hundred GeV and they can be detected at the LHC contrary to the original RS model with the bulk gauge fields. The bound on the physical mass scale is reduced to $\Lambda_\pi \lesssim 10$ TeV [27].

5 Universal extra dimensions (UED)

In this section we will discuss the scheme where all the SM fields propagate in the bulk and no walls are present. Due to the translation invariance in the higher dimensions and conservation of D-momentum, KK number n is conserved at the tree level. Namely, M different KK modes, n_1, n_2, \dots, n_M can couple to each other if the following relation holds

$$|n_1 \pm n_2 \dots \pm n_{M-1}| = n_M. \quad (22)$$

The interaction of the matter fields with the gauge fields is of the form

$$\mathcal{L} \sim c_{mnk} \bar{f}^{(m)} \gamma^\mu f^{(n)} A_\mu^{(k)}. \quad (23)$$

Although KK -number is broken at one loop level, the K -parity, $(-1)^n$, remains conserved [28]. It means that:

- KK excitations of the SM fields must be pair-produced at colliders
- lowest lying KK states of light quarks and gluons are stable

As we see, the K -parity reminds the R -parity in SUSY theories. Since the KK modes can no longer be produced as single resonances, we have a significant reduction of the collider sensitivity to their detection. The current experimental data put the limit $m_{KK} \gtrsim 300 - 400 \text{ GeV}$ [29, 28].

5.1 ACD scenario

The starting point of this approach [29] is the minimal SM in $D = 4 + d$ flat space-time dimensions. Let us consider the simplest case $d = 1$. In order to get chiral zero modes of fermions, an extra dimension has to be compactified on the orbifold S^1/Z_2 . All other fields can be classified then as either Z_2 even or odd. For instance, Higgs and gauge boson projections on 4D space are Z_2 even. The orbifold only admits the existence of the left-handed (right-handed) zero modes for the doublet (singlet) fermion fields.

At tree level, the masses of the KK excitations come mainly from 5D kinetic terms (with a small contribution from the Higgs):

$$m_n^2 = \frac{n^2}{R_c^2} + m_{SM}^2, \quad (24)$$

R_c being a compactification radius. Since R_c^{-1} is of the order of several hundred GeV, the KK states of the same level are almost degenerate in their masses. The real signature of the UED is a production of large number of heavy stable particles.

There are three classes of processes to be investigated at hadron colliders. The processes with color final states have the largest cross sections. they are mediated by the subprocess:

$$\begin{aligned}
qq' &\rightarrow q^{(1)}q'^{(1)}, \\
q\bar{q} &\rightarrow q^{(1)}\bar{q}^{(1)}, \\
gg + q\bar{q} &\rightarrow q'^{(1)}\bar{q}'^{(1)}, \\
gg &\rightarrow g^{(1)}g^{(1)}, \\
qq &\rightarrow q^{(1)}q^{(1)}.
\end{aligned} \tag{25}$$

The most significant subprocess is $qq' \rightarrow q^{(1)}q'^{(1)}$. The LHC will be able to probe the masses $m_{KK} \lesssim 3 \text{ TeV}$ [28]. The cross sections of the pair production of the lightest colored states are presented in Fig. 4.

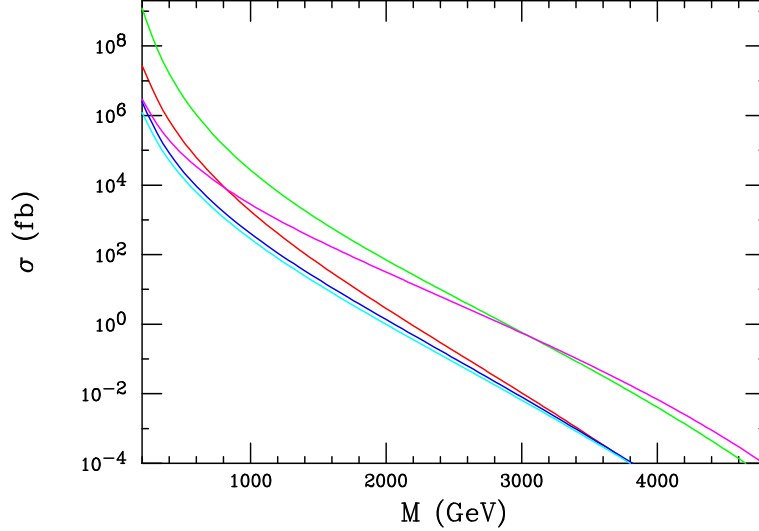


Figure 4: Cross section for the pair production of the lightest colored KK states at the LHC [28]. From top to bottom on the left-hand side, the curves correspond to the processes given in (25).

For the associated production of the lightest color singlet KK states $(g^{(1)}W^{(1)}, g^{(1)}Z^{(1)}, g^{(1)}\gamma^{(1)}, q^{(1)}W^{(1)}, q^{(1)}Z^{(1)}, q^{(1)}\gamma^{(1)})$, masses up to 1.5 TeV

can be detected. Finally, the production of color singlet states ($2Z^{(1)}Z^{(1)}$, $\gamma^{(1)}Z^{(1)}$, $2\gamma^{(1)}$, $W^{(1)+}W^{(1)-}$, $W^{(1)\pm}Z^{(1)}$, $W^{(1)\pm}\gamma^{(1)}$) will be probed at the LHC if $m_{KK} \lesssim 1.8 \text{ TeV}$ [28]. The limit on R_c^{-1} accessible on the LHC was estimated to be $13.5 - 15.5 \text{ TeV}$ [6].

At future e^+e^- colliders the KK excitation of the SM fields can be discovered in the processes $e^+e^- \rightarrow W^{(1)}W^{(1)}$, $2\gamma^{(1)}$, $Z^{(1)}\gamma^{(1)}$, $2Z^{(1)}$.

If the K -parity is conserved, the production of stable heavy KK particles will be missed at colliders. However, it can appear that a new physics makes them unstable. For instance, if the UED is embedded in a higher $(4 + d')$ -space with $d' > d$ and compactification radius $R'_c > R_c$, there are transitions of the form $KK(n=1) \rightarrow KK(n=0) + G$. Another possible way of violating the K -parity is to introduce an additional brane. The mixing between all KK excitations and zero mode results in then the transition $KK(n=1) \rightarrow 2KK(n=0)$, and the KK states can decay inside a detector (see [29] and [28] for details).

5.2 Bulk fermions in RS background

As we already know, the KK excitations of the gauge fields are significantly lighter than the corresponding KK excitations of the graviton. In Ref. [32] the masses of the bulk fermions were found to be $m_n^f = n\pi k / [\exp(\pi k r_c) - 1]$.

In a consequent paper [15], the Dirac 5D mass term required by the Z_2 orbifold symmetry was introduced in the action. For simplicity all fermions are taken to have the same mass $m = \nu k$, where ν is an arbitrary parameter. In such a scheme the masses of the KK excitations have an approximately linear dependence on ν :

$$m_n^f = a_n |\nu + 1/2| + b_n, \quad (26)$$

a_n , b_n being some constants. The KK fermion states are expected to be more massive than the corresponding KK states of the gauge bosons [15]. In the rest of this section we consider this model.

The couplings of the resulting KK states strongly depend on the value of ν . For instance, the ratio g_n/g is quite small for $\nu \lesssim -0.5$, while for $\nu \gg 1$ the result for the RS approach with the wall fermions (21) is reproduced.

The phenomenology of the model is determined by the parameters k , Λ_π and ν . The primary discovery mode for the gauge bosons at hadron colliders could be Drell-Yan process ($p\bar{p} \rightarrow \gamma^{(1)}/Z^{(1)} \rightarrow l^+l^-$), but it gives no new

signature. Unfortunately, both the W^+W^- -fusion and the top production are also poor places to search for KK events [33]. Thus, it seems unlikely that the KK excitations will be produced directly at the LHC [33, 34].

As for future linear colliders, the range $m_1 \lesssim 15$ TeV can be probed for $\nu \lesssim -0.3$ in $e^+e^- \rightarrow \gamma^{(1)}/Z^{(1)} \rightarrow f\bar{f}$ ($f = e, \mu, \dots, t$), if center-of-mass energy $\sqrt{s} = 500 - 1000$ GeV and integrated luminosity $\mathcal{L} = 500 - 1000 \text{ fb}^{-1}$ are obtained [33].

6 Minimal universal extra dimension (MUED)

This model proposed in Refs. [35] is defined in five dimensions with an additional dimension compactified on the S^1/Z_2 as in the UED. The full Lagrangian of the MUED contains both bulk and boundary interactions. The latter are localized at the fixed points of the orbifold, and, thus, do not respect 5D Lorentz invariance. The boundary terms are chosen to be symmetric under the exchange of the orbifold fixed points, and the K -parity remains an exact symmetry.

These new interactions:

- violate the KK number by even units
- lead to a mass splitting between the KK modes
- affect their decays

The boundary term are assumed to be small at some scale $\Lambda > R_c^{-1}$.

There are only three free parameters in the MUED: R_c , Λ and m_h , where m_h is the mass of the SM Higgs. The dependence of the splitting between KK excitation with $n = 1$ on the scale Λ (at fixed $R_c^{-1} = 500$ GeV and $m_h = 120$ GeV) has been calculated in [35]. The corrections to the masses are such that the heaviest (lightest) particle is the first KK states of the gluon (photon). The $SU(2)$ doublet quarks, $Q^{(1)}$, are heavier than singlet quarks, $q^{(1)}$.

The collider phenomenology of the first KK level is very similar to the SUSY scheme in which the superpartners are close in their masses (with $\Delta m = 100 - 200$ GeV). Like the LSP is stable in R -parity conserving SUSY, the lightest KK particle (LKP), $\gamma^{(1)}$, is stable due to the K -parity conservation. The KK spectroscopy and possible transitions in the MUED is shown in Fig. 5.

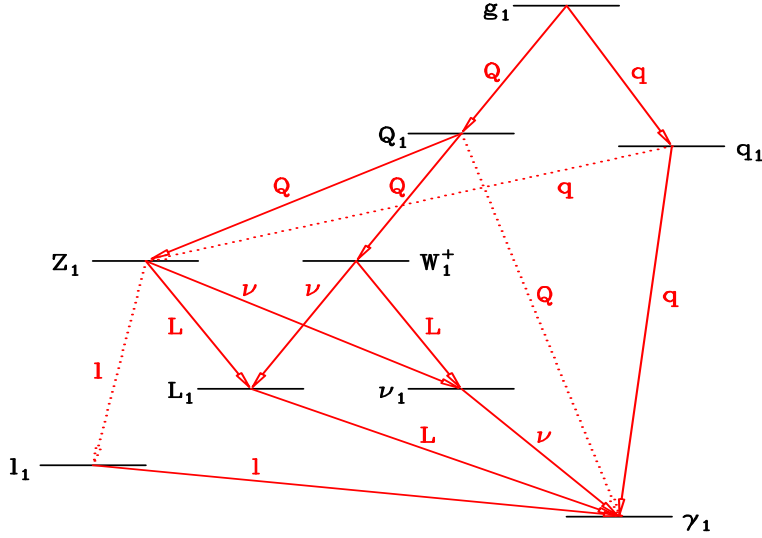


Figure 5: Qualitative sketch of the level 1 KK spectroscopy depicting the dominant (solid) and rare (dotted) transitions and the resulting decay product [35].

At hadron coliders the KK states are pair-produced. The process with the largest rate is $pp \rightarrow N\text{jet} + \cancel{E}$ ($N \geq 2$). It is mediated by an inclusive production of $q^{(1)}\bar{q}^{(1)}$ and it is similar to the usual squark (sgluino) search. The measured missing energy is rather small. The LHC is expected to reach only mass scales up to $R_c^{-1} \lesssim 1.2 \text{ TeV}$ [35]. The more promising process is an inclusive production of $Q^{(1)}\bar{Q}^{(1)}$ -pair with the subsequent decays of the quark KK excitations into leptonic final states. As a result, we have a signature $4l + \cancel{E}$. The main background comes from the subprocess $Z(\gamma)Z(\gamma) \rightarrow l^\pm l^\mp \tau^+ \tau^- \rightarrow 4l + \cancel{E}$ (Z and γ may be real or virtual). The scale $R_c^{-1} \sim 1.5 \text{ TeV}$ can be reached. Another channels with two or three leptons in the final state have larger backgrounds.

We have already seen that MUED signals may be easily confused with the SUSY signals. It is a linear collider that can help us to distinguish the MUED from SUSY. One such a possibility is the production of KK electrons in e^-e^- collisions [36]. As for the LHC, one has to look for the existence of the KK modes with $n \geq 2$ which should be the smoking gun signature for the MUED.

7 Radion

7.1 Graviscalar-Higgs mixing

Let us analyze scalar content of the ADD scheme with d additional compact flat dimensions which was considered in Section 2. The KK tower of a 5D gravitational field h_{AB} ($A, B = 0, 1, \dots, 4+d$) contains a set of gauge-invariant fields of different spin: $G_{\mu\nu}^{(n)}$, $V_{\mu i}^{(n)}$, $S_{ij}^{(n)}$ and $H^{(n)}$, where indexes i, j run over extra dimensions. From the point of view of four dimensions, $G_{\mu\nu}^{(n)}$ is the massive spin-two particle (n -th KK excitation of the graviton). Both vector fields, $V_{\mu i}^{(n)}$, and massive real scalars, $S_{ij}^{(n)}$, are not coupled to the matter and play no roles in a phenomenology. The scalars $H^{(n)}$ are coupled only to the trace of the energy-momentum tensor [8]:

$$\mathcal{L}_{int} = -\frac{\kappa}{3\bar{M}_{Pl}} \sum_n H^{(n)} T_\mu^\mu, \quad (27)$$

where $\kappa = \sqrt{3(d-1)/(d+2)}$.

For $d = 1$, only zero massless mode of $H^{(n)}$, called radion, is present, while KK excitations of the radion are eaten by the massive gravitons. The radion corresponds to fluctuations of the volume of the extra dimension. There exist several mechanisms which stabilize the radius of the extra dimension and give a mass to the radion (see, for instance, [37]). At $d > 1$, there is a tower of massive graviscalars.

At tree level the coupling of the scalars to the massless fermions and gauge bosons vanishes, as one can see from (27). However, the graviscalars may play an important role if there is a scalar fields, φ , living on the brane. The point is that one can add the following 4D term, involving the Ricci scalar R , to 4D effective Lagrangian

$$\Delta\mathcal{L} = -\xi R\varphi^+, \quad (28)$$

with a free parameter ξ . In the unitary gauge, φ is reduced to the physical Higgs via the relation $\varphi = (v+h, 0)/\sqrt{2}$, v being the VEV of the Higgs field.

Taking into account (27) and (28), we get graviscalar-Higgs mixing term of the form [38]

$$\mathcal{L}_{mix} = \frac{2\kappa\xi vm_h^2}{\bar{M}_{Pl}} h \sum_n H^{(n)}. \quad (29)$$

As it has been shown in [38], an oscillation of the Higgs field into a huge number ($\sim \bar{M}_{Pl}^2$) of closely spaced scalars is equivalent to a decay of the Higgs on collider time scale with partial width

$$\Gamma \sim \pi \kappa \xi^2 v^2 \frac{m_h^d}{M_D^{2+d}}. \quad (30)$$

This width corresponds to the invisible decay of the Higgs, since the graviscalars will escape a detector.

The search for the invisible decay at the LHC could help us to discover the Higgs provided its mass is below 250 GeV. At e^+e^- collider with the energy $\sqrt{s} = 500$ GeV and integrated luminosity $\mathcal{L} = 200 \text{ fb}^{-1}$, the range $80 < m_h < 170$ GeV can be probed [38].

7.2 Radion in RS model

In the RS model (see Section 3) the radion field arises as an excitation of the volume of the slice of the AdS_5 space, $r_c \rightarrow T(x)$. In terms of the dynamical field $T(x)$, the metric of the model (11) may be presented in the form

$$ds^2 = e^{-2k|\theta|T(x)} \eta_{\mu\nu} dx^\mu dx^\nu + T^2(x) d\theta^2. \quad (31)$$

Let us introduce more conventional definition $\phi = \Lambda_\phi e^{-k\pi(T-r_c)}$. Here $\Lambda_\phi = \sqrt{24M_5^3/k} \exp(-k\pi r_c)$ and M_5 is the 5D Planck scale. Due to a mechanism stabilizing the size of the extra dimension (see, for instance, [39, 40]), the radion ϕ acquires a dynamical mass of the order of 1 TeV or less. The common expectation is that the radion may be the lightest new particle in the RS model.

The interaction of the radion ϕ with the SM fields located on the brane is given by

$$\mathcal{L}_{int} = -\frac{\phi}{\Lambda_\phi} T_\mu^\mu. \quad (32)$$

The radion phenomenology is very similar to the SM Higgs up to the rescaling factor v/λ_ϕ , except that its couplings to two photons and gluons are enhanced by the trace anomaly. The $\phi\phi h$ coupling can be substantially larger than the hhh coupling [41].

Relatively light radion decays dominantly into two gluons (the decay is enhanced by the gluon anomaly presented in T_μ^μ) contrary to the SM Higgs

which decays into $b\bar{b}$ pair. If the radion mass lies within the limits $150 \lesssim m_\phi \lesssim 2m_W$, the main mode will be $\phi \rightarrow hh$ (if kinematically allowed). The heavier radion decays into W^+W^- and ZZ .

Let us consider first the detection of the radion when it does not mix with the Higgs. At hadron colliders the production subprocesses are $gg \rightarrow \phi$ (the most important channel), $q\bar{q}' \rightarrow W\phi$, $q\bar{q} \rightarrow Z\phi$, $qq' \rightarrow qq'\phi$ and $q\bar{q}$, $gg \rightarrow t\bar{t}\phi$ [42]. The cross section can be seen in Fig. 6.

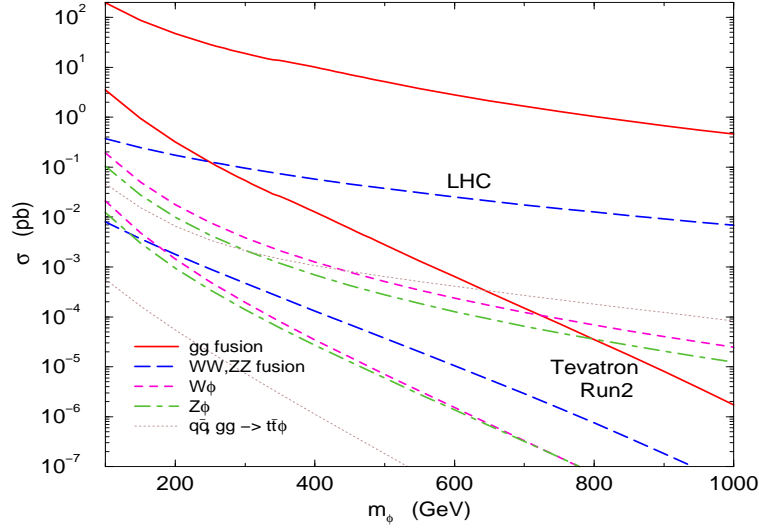


Figure 6: Production cross sections versus m_ϕ for $p\bar{p} \rightarrow \phi$ (gg fusion), $p\bar{p} \rightarrow qq'\phi$ (WW, ZZ fusion), $p\bar{p} \rightarrow W\phi$, $p\bar{p} \rightarrow Z\phi$, and $p\bar{p} \rightarrow t\bar{t}\phi$ [42].

The dijet production ($gg \rightarrow \phi \rightarrow gg$) has too large background and a signal is about 1% at the LHC. The $b\bar{b}$ mode is not also a good place for a radion detection, as the corresponding branching is ten times smaller than that of the SM Higgs. For rather heavy radion ($m_\phi > 180$ GeV) the cleanest signature is [38, 42]

$$gg \rightarrow \phi \rightarrow ZZ \rightarrow 4l. \quad (33)$$

The radion has a smaller width than the Higgs. Thus, one has to search for a small invariant mass of four leptons in (33). The LHC can reach $m_\phi \lesssim 1$ GeV. In the WW mode ($gg \rightarrow \phi \rightarrow WW \rightarrow l\bar{l}\nu\bar{\nu}$) the radion can be defined in the mass range $m_\phi = 140 - 190$ GeV if $\Lambda_\phi \simeq v$ [42].

At linear colliders, the radion can be produced in $e^+e^- \rightarrow Z\phi$, $\nu\bar{\nu}\phi$, $e^+e^-\phi$. The search strategy should be similar to that of the Higgs, but with

the detection of two jets instead of $b\bar{b}$ -pair in final states.

The radion-Higgs mixing induced by the term (28) shifts the properties of both fields [38, 43] which become dependent on a mixing parameter ξ . For instance, the branching fraction $h \rightarrow gg$ can be strongly modified with respect to its SM expectation [44]. The case $\xi = 1/6$ ("half Higgs, half radion") is the special one. The coupling of ϕ to the fermions, W and Z are suppressed for $\xi = 1/6$ and the gg -branching of the radion dominates for all values of m_ϕ [38]. In Ref. [38] the search capability of the LHC has been estimated:

- $110 < m_\phi \leq 150 \text{ GeV}$ ($2 \lesssim \Lambda_\phi \lesssim 3 \text{ TeV}$)
- $150 < m_\phi \leq 550 \text{ GeV}$ ($3 \lesssim \Lambda_\phi \lesssim 7 \text{ TeV}$)
- $550 < m_\phi \leq 950 \text{ GeV}$ ($4 \lesssim \Lambda_\phi \lesssim 7 \text{ TeV}$)

The radion properties in the RS scenario where the SM field propagate in the bulk, were considered in [43]. It was shown that there is no differences in $f\bar{f}$, hh modes, but massless modes are seriously modified. Namely, the width $\Gamma(\phi \rightarrow gg)$ receives 40–50% increase and the width $\Gamma(\phi \rightarrow gg)$ changes even more drastically.

8 Black holes at colliders

8.1 Black hole production

As we know from Section 2, the 5D Planck scale, at which the gravity becomes strong, is $M_D \sim 1 \text{ TeV}$ for $D = 10$. If this scenario is realized in nature, a production of black holes should be possible at super-Planckian energies ($\sqrt{s} \gg 1 \text{ TeV}$). Black hole intermediate states are expected to dominate s -channel scattering. Indeed, in the string theory the number of such states grows with black hole mass, M_{BH} , faster than the number of perturbative states [45]. Moreover, as we will see below, the cross section of the black hole production rises in \sqrt{s} more rapidly than in processes associated with the perturbative physics.

The Schwartzchild radius of a $(4 + d)$ dimensional black hole with the mass M_{BH} depends on its spin J . For $J = 0$ it is given by [46]

$$R_S(M_{BH}) = \frac{1}{M_D} \left(\frac{M_{BH}}{M_D} \right)^{1/(1+d)}. \quad (34)$$

In what follows, it is assumed that

$$R_S \ll R_c, \quad (35)$$

where R_c is a characteristic geometrical scale of the model. In addition, the black hole masses larger than the tension are only considered. These two assumptions mean that we can use flat space formulae.

Then the black hole can be considered as a neutral spinning solution of the D dimensional Einstein action with the radius R_S (34), the Hawking temperature

$$T_H \xrightarrow{J \rightarrow 0} \frac{d+1}{4\pi R_S} \quad (36)$$

and the entropy

$$S_{BH} \xrightarrow{J \rightarrow 0} \text{const} (R_S M_D)^{d+2}, \quad (37)$$

where the constant in the RHS of Eq. (37) depends on d .

It is necessary to define the applicability of the description of the black hole as a massive semi-classical state. The main quantum corrections are due to the change in the Hawking temperature (36) per particle emission. The condition that back-reaction of this emission on the black hole to be small is equivalent to $S_{BH} \gg 1$. Another criteria is the validity of the statistical description for the black hole, that results in the inequality $\sqrt{S_{BH}} \gg 1$ [45]. The value of $S_{BH} \gtrsim 25$ is usually taken, which means $M_{BH} \gtrsim 5M_D$. As for classical modifications of gravity (string corrections), the corresponding effects can be neglected if $R_S > M_s$, where M_s is the string scale.

Let us consider two colliding objects with the energy \sqrt{s} . If an impact parameter b becomes smaller than some critical value (which is of the order of the Schwartzchild radius $R_S(s)$ (34)), the black hole is formed. As $R_S(s)$ is large and grows with energy, the production of the black hole can be described by classical General Relativity [47].

So, at $b \leq R_S(s)$, the scattering is dominated by “resonant” production of a single black hole with $M_{BH} = \sqrt{s}$. It is important to note that the event horizon of colliding particles forms long before their collision takes place. In hadron-hadron scattering the cross section of the black hole production is of the form

$$\sigma_{pp \rightarrow BH}(s) = \sum_{a,b} \int_{\tau_{min}}^1 d\tau \int_{\tau}^1 \frac{dx_a}{x_a} f_a(x_a) f_b\left(\frac{\tau}{x_a}\right) \sigma_{ab \rightarrow BH}(\tau s). \quad (38)$$

Here $\tau_{min} = M_{BH}^{min}/s$ and the black hole mass is assumed to be $M_{BH} \simeq \sqrt{\tau s}$. Following Thorne's hoop conjecture, the cross section of two partons, a and b , are taken in a simple geometric form [45]:

$$\sigma_{ab \rightarrow BH}(s) \approx \pi R_S^2(s). \quad (39)$$

Recent calculations (see, for instance, [48]) indicate that quantum corrections to the semi-classical expression (39) are small.

As we can see, the cross section has no small coupling constants and it rises rapidly with the energy, while hard perturbative processes are highly suppressed above the scale M_D . The summation over all types of initial partons in (38) results in an additional enhancement of the black hole production. Once the black hole is formed, colliding particles never get close enough to perform a hard scattering. With TeV scale gravity, the production of the black holes should be a dominant process at the LHC. The total cross section can be as large as 0.5 (120) fb for $M_{BH} = 2$ (6) TeV and $d = 7$ (3) [49].

8.2 Black hole decays

The black hole decay occurs in several stages. The first stage is so-called balding phase, where highly asymmetrical black hole performs classical gauge and gravitational radiation. As a result, the black hole with no hair is produced. One expects that the black hole emits 16% of its mass.

The black hole is formed with rather large spin $J \sim R_S M_{BH}$. In spin-down phase it is shed in quanta with angular momentum $L \sim 1$ and energy $E \sim R_S^{-1}$. About 25% of the black hole's energy is radiated during this phase.

The remaining energy of the black hole is mainly lost in a Schwarzschild phase. At this stage, the black hole's evaporation is a thermal (grey body) emission at Hawking temperature (36). It is important that the black hole decays visibly to the SM particles living on the brane [50]. The total number of emitted particles is equal to $\langle N \rangle \simeq M_{BH}/T_H$. The typical black hole's lifetime is $\tau_{BH} \sim 10^{-26}$ sec, which corresponds to the total width $\Gamma_{BH} \sim 10$ GeV [49].

Finally, the black hole with a mass $M_{BH} \sim M_D$ decays into several quanta with energies $O(M_D)$. This decay is called Planck phase.

The experimental signatures of the black hole production are very distinctive:

- flavor-blind (thermal) decays

- hard prompt charged leptons and photons (with energy $E \gtrsim 100$ GeV)
- the ratio of hadronic to leptonic activity is closed to 5 : 1 [45]
- complete cut-off of hadronic jets with $p_{\perp} > R_S^{-1}$ [47]
- the small missing energy

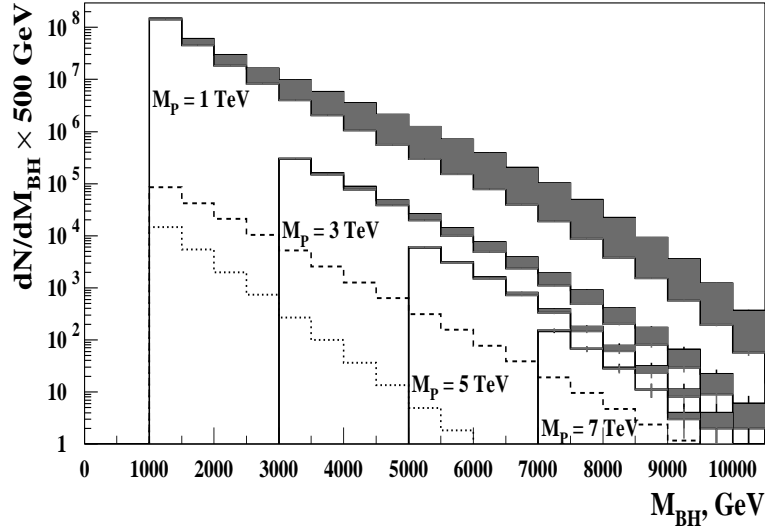


Figure 7: Number of black holes produced at the LHC in the electron or photon decay channels, with $\mathcal{L} = 100 \text{ fb}^{-1}$, as a function of M_{BH} . The shaded regions correspond to the variation in the number of events for d between 2 and 7. The dashed line shows total SM background (from inclusive $Z(ee)$ and direct photon production). The dotted line corresponds to the $Z(ee) + X$ background alone [49].

These signatures (considered together) have almost vanishing SM background. The LHC discovery potential is maximized in $e/\mu + X$ channel. The multiplicity distribution of the black holes produced is presented in Fig. 7. The SM backgrounds from $Z(e^+e^-) + \text{jet}$ or $\gamma + \text{jet}$ final states are small and scales up to $M_D \lesssim 9 \text{ TeV}$ can be reached [49]. The production cross sections of black holes were also calculated in [51].

If the dependence of the Hawking temperature T_H vs. M_{BH} will be measured, one can determine the number of the extra dimensions by taking the

logarithm of both sides of Eq. (36):

$$\log T_H = -\frac{1}{d+1} \log M_{BH} + \text{const}, \quad (40)$$

where the constant depends only on M_D , but not on d .

However, the evaporation of the black hole may significantly change in models with separated fermions, once R_S is smaller than the separation distance [52]. Then the ratio of jets to charged leptons and photons becomes $113 : 8 : 1$. The spin of the black hole also affects energy and angular spectra of the Hawking radiation [53]. Moreover, some authors argue that D -dimensional black hole must radiate mainly into KK modes [54, 47]. Note that the key geometric formula (39) needs more justification as well.

9 Conclusions

The LHC will be able to detect signals from higher-space dimensions and to reach the effective Planck scale up to $5 - 10$ TeV, depending on the model and the experimental signature. The e^+e^- collisions should be effective in the indirect search for the KK excitations. In the scheme with non-factorizable metric, the masses of KK states as large as several ten TeV can be probed at the linear collider with energy $\sqrt{s} = 1$ TeV and integrated luminosity $\mathcal{L} = 500 \text{ fb}^{-1}$.

Acknowledgments

I am grateful to the Organizing Committee of the Workshop for suggesting me a subject for my review talk and to V.A. Petrov for stimulating discussions.

References

- [1] T. Kaluza, Sitzungsber. Preuss. Akad. Wiss. Berlin (Math. Phys.) **K1**, 966 (1921); O. Klein, Z. Phys. **37**, 895 (1926).
- [2] I. Antoniadis, Phys.Lett. **B246**, 377 (1990); I. Antoniadis, K. Benakli, Phys.Lett. **B326**, 69 (1994).

- [3] N. Arkani-Hamed, S. Dimopoulos and G. R. Dvali, Phys. Lett. **B429**, 263 (1998); I. Antoniadis, N. Arkani-Hamed, S. Dimopoulos and G. R. Dvali, Phys. Lett. **B436**, 257 (1998); N. Arkani-Hamed, S. Dimopoulos and G. R. Dvali, Phys. Rev. **D59**, 086004 (1999).
- [4] V.A. Rubakov, Phys. Usp. **44**, 871 (2001); Yu.A. Kubyshin, *Lectures given at the XI School "Particles and Cosmology"*, Baksan, Russia, 18-24 April, 2001.
- [5] J. Hewett and M. Spiropulu, preprint hep-ph/0205106 (2002) (submitted to Annual Review of Nuclear and Particle Sciences).
- [6] G. Azuelos *et al.*, *Proceedings of the Workshop "Physics at TeV Colliders"*, Les Houches, France, 21 May - 1 June 2001.
- [7] T. Han, J. Lykken and R.-J. Zhang, Phys. Rev. **D59**, 105006 (1999).
- [8] G. F. Giudice, R. Rattazzi and J. D. Wells, Nucl. Phys. **B544**, 3 (1999).
- [9] J. L. Hewett, Phys. Rev. Lett. **82**, 4765 (1999).
- [10] T.G. Rizzo, preprint hep-ph/0208027 (2002).
- [11] L. Randall and R. Sundrum, Phys. Rev. Lett. **83**, 3370 (1999).
- [12] L. Randall and R. Sundrum, Phys. Rev. Lett. **83**, 4690 (1999); J. Lykken and L. Randall, JHEP **06**, 014 (2000).
- [13] H. Davoudiasl, J.L. Hewett and T.G. Rizzo, Phys. Rev. Lett. **84**, 2080 (2000).
- [14] B.C. Allanach *et al.*, JHEP **0009**, 019 (2000).
- [15] H. Davoudiasl, J.L. Hewett and T.G. Rizzo, Phys. Rev. **D63**, 075004 (2001).
- [16] A. Pomarol and M. Quir  s, Phys. Lett. **B438**, 255 (1998).
- [17] M. Masip and A. Pomarol, Phys. Rev. **D60**, 096005 (1999).
- [18] T.G. Rizzo and J.D. Wells, Phys. Rev. **D61**, 016007 (2000).
- [19] I. Antoniadis, K. Benakli and M. Quir  s, Phys.Lett. **B331**, 313 (1994).

- [20] R. Casalbuoni *et al.*, Phys. Lett. **B462**, 48 (1999); P. Nath, Y. Yamada and M. Yamaguchi, Phys. Lett. **B466**, 100 (1999); A. Strumia, Phys. Lett. **B466**, 107 (1999); F. Cornet, M. Relaño and J. Rico, Phys. Rev. **D61**, 037701 (2000); C.D. Carone, Phys. Rev. **D61**, 015008 (2000).
- [21] T.G. Rizzo, Phys. Rev. **D61**, 055005 (2000).
- [22] I. Antoniadis, K. Benakli and M. Quirós, Phys. Lett. **B460**, 176 (1999).
- [23] A. Pomarol, Phys. Lett. **B486**, 153 (2000).
- [24] H. Davoudiasl, J.L. Hewett and T.G. Rizzo, Phys. Lett. **B473**, 43 (2000).
- [25] C. Csáki, J. Erlich and J. Terning, Phys. Rev. **D66**, 064021 (2002).
- [26] H. Davoudiasl, J.L. Hewett and T.G. Rizzo, preprint hep-ph/0211377 (2002).
- [27] H. Davoudiasl, J.L. Hewett and T.G. Rizzo, preprint hep-ph/0212279 (2002).
- [28] T. Rizzo, Phys. Rev. **D64**, 095010 (2001).
- [29] T. Appelquist, H-C. Cheng and B.A. Dobrescu, Phys. Rev. **D64**, 035002 (2001).
- [30] J. Lykken and S. Nandi, Phys. Lett. **B485**, 224 (2000).
- [31] D.A. Dicus, C.D. McMullen and S. Nandi, Phys. Rev. **D65**, 076007 (2002).
- [32] S. Chang *et al.*, Phys. Rev. **D62**, 0840025 (2000).
- [33] J.L. Hewett, F.J. Petriello and T.G. Rizzo, JHEP **0209**, 030 (2002).
- [34] S.J. Huber, C-A. Lee and Q. Shafi, Phys. Lett. **B531**, 112 (2002); G. Burdman, Phys. Rev. **D66**, 076003 (2002).
- [35] H-C. Cheng, K. Matchev and M. Schmaltz, Phys. Rev. **D66**, 036005 (2002); *ibid.* **D66**, 056006 (2002).

- [36] H-C. Cheng, *Talk at the 4-th Int. Workshop on Electron-Electron Interaction at TeV Energies*, University of California, Santa Cruz, 7-9 December, 2001.
- [37] N. Arkani-Hamed, S. Dimopoulos and J. March-Russell, Phys. Rev. **D63**, 064020 (2001).
- [38] G. F. Giudice, R. Rattazzi and J. D. Wells, Nucl. Phys. **B595**, 250 (2001).
- [39] W.D. Goldberger and M.B. Wise, Phys. Rev. Lett. **83**, 4922 (1999).
- [40] C. Csáki *et al.*, Phys. Rev. **D62**, 045015 (2000); C. Csáki, M. Graesser and G.D. Kribs, *ibid.* **D63**, 064020 (2001).
- [41] A. Bae, P. Ko and H.S. Lee, Phys. Lett. **B487**, 299 (2000).
- [42] K. Cheung, Phys. Rev. **D63**, 056007 (2001).
- [43] T.G. Rizzo, JHEP **0206**, 056 (2002).
- [44] T.G. Rizzo, preprint hep-ph/0207113 (2002).
- [45] S.B. Giddings and S. Thomas, Phys. Rev. **D65**, 056010 (2002); S.B. Giddings, preprint hep-ph/0110127 (to appear in the Proc. of “Snowmass 2001”).
- [46] R.C. Myers and M.J. Perry, Ann. Phys. **172**, 304 (1986).
- [47] T. Banks and W. Fisher, preprint hep-th/9906038 (1999).
- [48] D.M. Eardley and S.B. Giddings, Phys. Rev. **D66**, 044011 (2002); S.D.H. Hsu, Phys. Lett. **B555**, 92 (2003).
- [49] S. Dimopoulos and G. Landsberg, Phys. Rev. Lett. **87**, 161602 (2001).
- [50] R.E. Emparan, G.T. Gorowitz and R.C. Myers, Phys. Rev. Lett. **85**, 499 (2000).
- [51] K. Cheung, Phys. Rev. **D66**, 036007 (2002).
- [52] T. Han, G.D. Kribs and B. McElrath, Phys. Rev. Lett. **90**, 031601 (2002).

- [53] A.V. Kotwal and C. Hays, Phys. Rev. **D66**, 116005 (2002).
- [54] P. Argyres, S. Dimopoulos and J. March-Russel, Phys. Lett. **B441**, 96 (1998).